Supplementary Results

1. Alterations in AI of structural morphological metrics in AD.

Compared the gray matter volume asymmetry index (AI) across multiple brain regions among patients with Alzheimer's Disease (AD), Mild Cognitive Impairment (MCI), and Normal Control (NC) subjects. Statistical analyses (FDR-corrected) revealed that the AD group exhibited significant alterations in AI compared to the NC group in numerous brain regions, with effect sizes (Cohen's d) ranging from -0.548 to 0.720. Specifically, within the frontal lobe, the AD group showed significant differences in the inferior frontal gyrus, opercular part (IFG, A44op, Cohen's d = -0.359, p-FDR < 0.001) and the middle orbital gyrus (OrG, A14m, Cohen's d = 0.321, p-FDR = 0.003). In the temporal lobe, significant differences between AD and NC were identified in several regions, including the superior temporal gyrus (STG, A22c, Cohen's d = -0.548, p-FDR = 0.003), inferior temporal gyrus (ITG, A20iv, Cohen's d = -0.243, p-FDR = 0.041), fusiform gyrus (FuG, A37lv, Cohen's d = 0.272, p-FDR = 0.027), and parahippocampal gyrus (PhG, A35_36r). Notably, the posterior superior temporal sulcus (PSTS, cpSTS, Cohen's d = -0.361, p-FDR = 0.050) and the postcentral gyrus (PoG, A2, Cohen's d = -0.237, p-FDR = 0.047) demonstrated significant alterations not only in the AD vs. NC comparison but also in the direct comparison of AD vs. MCI. Among the subcortical nuclei, the most pronounced difference was observed in the hippocampus (Hipp, cHipp), which yielded a large positive effect size (Cohen's d = 0.720, p-FDR < 0.001) in the AD-NC comparison and a medium-to-large effect (Cohen's d = 0.560, p = 0.002) in the AD and MCI comparison. Furthermore, two subregions of the thalamus (PPtha and Otha) also showed significant differences between AD and NC groups (For PPtha: Cohen's d = 0.438, p-FDR = 0.027; For Otha: Cohen's d = 0.428, p-FDR = 0.003). No brain regions showed significant differences in GMV between the MCI and NC groups, after FDR correction.

For AI of FD, AD showed only three brain regions with significant differences, compared to NC. Specifically, within the temporal lobe, the superior temporal gyrus (STG, A22c and A22r, Supplementary Fig. 2 and Supplementary Table 2) exhibited a rightward asymmetry, with a negative effect size (For A22c: Cohen's d = -0.394, p-FDR = 0.032; For A22r: Cohen's d = -0.355, p-FDR = 0.022), respectively. In contrast, the parahippocampal gyrus (PhG, A35_36r) in the temporal lobe showed a leftward asymmetry, with a positive effect size (Cohen's d = 0.526, p-FDR < 0.001). In the comparison between the AD and MCI groups, significant differences were observed in more regions. Within the frontal lobe, the orbital gyrus (OrG, A11l) and paracentral lobule (PCL, A4ll) both showed a leftward asymmetry, with a significant positive effect size (For A11l: Cohen's d = 0.292, p-FDR = 0.040; For A4ll: Cohen's d = 0.359, p-FDR = 0.005). Furthermore, other regions—including the temporal lobe (STG A22c and PhG A37lv), limbic lobe (CG A23v), and occipital lobe (MVOCC vmPOS)—generally showed a greater rightward asymmetry. No brain regions showed significant differences in FD between the MCI and NC groups, after FDR correction.

For AI of CT, there were 4 regions showed significant group differences between AD and NC, after FDR correction. There were Inferior Frontal gyrus and Orbital gyrus. All of them showed exhibited a significant increase in rightward asymmetry in AD, with a significant negative effect (Supplementary Fig. 3 and Supplementary Table 3; For A44op: Cohen's d = -0.299, p-FDR = 0.022; For A14m: Cohen's d = -0.326, p-FDR = 0.020; For A11l: Cohen's d = -0.360, p-FDR = 0.013; For A12_47l: Cohen's d = -0.298, p-FDR = 0.039). No brain regions showed significant differences in CT between the AD and MCI groups, after FDR correction. No brain regions showed significant differences in CT between the MCI and NC groups, after FDR correction.

For AI of GI, there was only one single brain region left after FDR correction in the comparison between AD and NC groups. This region was the superior temporal gyrus (Supplementary Fig. 4 and Supplementary Table 4; STG, A3l), which exhibited a significant increase in rightward asymmetry in AD, with a significant negative effect (Cohen's d = -0.320, p-FDR = 0.026). No brain regions showed significant differences in GI between the AD and MCI groups, after FDR correction. No brain regions showed significant differences in GI between the MCI and NC groups, after FDR correction.

For AI of SD, there was only one single brain region left after FDR correction between AD and NC groups. This region was the superior parietal gyrus (SPL, A7c; Supplementary Fig. 5 and Supplementary Table 5), which exhibited a significant decrease in leftward asymmetry in AD, with a significant negative effect (Cohen's d = -0.331, p-FDR = 0.016, Supplementary Fig. 5 and Supplementary Table 5). No brain regions showed significant differences in SD between the AD and MCI groups, after FDR correction. No brain regions showed significant differences in SD between the MCI and NC groups, after FDR correction.

2. Alterations in HFC and the AI of structural morphological metrics in MCI.

There were no significant differences between MCI and HC in the HFC after FDR correction, as showed in Figure 2d. There was no region showed significant group differences between MCI and HC in AI of any of structural morphological metrics, after FDR correction, as showed in Supplementary Figure 1d, Supplementary Figure 2d, Supplementary Figure 3d, Supplementary Figure 4d and Supplementary Figure 5d.

3. Model performance under different feature selection schemes in classification task distinguishing AD from MCI.

In the binary classification task distinguishing AD from MCI, the HFC represents a robust neuroimaging biomarker. Specifically, the model utilizing whole-brain HFC features achieved an averaged ACC of 0.653 via leave-one-site out cross-validation (Supplementary Fig. 7c). The HFC showed the highest accuracy (ACC = 0.653) among all single-modality models, outperforming all structural morphological metrics including GMV (ACC = 0.624), FD (ACC = 0.571), CT (ACC = 0.596), GI (ACC = 0.530), SD (ACC = 0.517). When utilizing regions with significant alteration of HFC both after FDR corrected or not in either AD group or MCI groups as features, the model's accuracy remained essentially constant, exhibiting only a marginal drop (For sig-brains: ACC = 0.621; For FDR-brains: ACC = 0.613) (Supplementary Fig. 7c). This trend was consistent for both F1 score and AUC (Supplementary Fig. 7c). During leave-one-site-out cross-validation, the model achieved site-specific accuracies ranging from 0.507 to 0.800, indicating variable performance across data sources (Supplementary Fig. 7a). The evaluate metrics for each site could be seen in Supplement Table S9. The ROC curves of the model were shown in Supplementary Fig. 7b.

Like the classification task of distinguishing AD from NC, the integration the HFC features with the AI features of the structural metrics also enhanced classification performance with an average margin of 6.12% for structural metrics (Supplementary Fig. 7c), suggesting that functional network information can provide valuable complementary data for improving diagnostic accuracy.

4. Model performance under different feature selection schemes in prediction clinical cognitive scores for AD and MCI.

HFC showed the potential as a robust neuroimaging biomarker to predict the clinical cognitive scores via leave-one-site-out cross-validation for AD and MCI. Specifically, the model utilizing whole-brain HFC as features achieved an average correlation of 0.288 between the predicted and actual MMSE scores via leave-one-site out cross-validation (Supplementary Fig. 8), outperforming the AI of several single-structural metrics including FD (r =0.202), GI (r = 0.147) and SD (r = 0.101). However, HFC showed lower predictive performances compared to GMV (r = 0.435) and CT (r =0.302). Notably, the predictive performance remained stable when using only regions showing significant HFC alterations in AD or MCI. The correlation only marginally decreased when restricting features to FDR-corrected significant regions (r = 0.233) or uncorrected significant regions (r = 0.241), indicating the robustness of HFC features.

Consistent with the classification task, the integration of HFC with structural metrics through multi-modal fusion led to improved performance in classifying AD from MCI. Specifically, the fusion of HFC with GMV model achieved the highest performance (r = 0.492, MAE = 4.618, RMSE = 5.678), while the union of HFC with CT also showed noticeable improvement (r = 0.398, MAE = 4.897, RMSE = 6.049). For the structurally weaker metrics FD, GI, and SD, the incorporation of HFC features resulted in substantial performance gains, with correlation increases of approximately 0.1, confirming the complementary value of HFC in multi-modal frameworks. The site-specific performance variations and detailed evaluation metrics for each site are provided in Supplementary Table S11, with corresponding visualization in Supplementary Figure S8.

Supplementary Figures

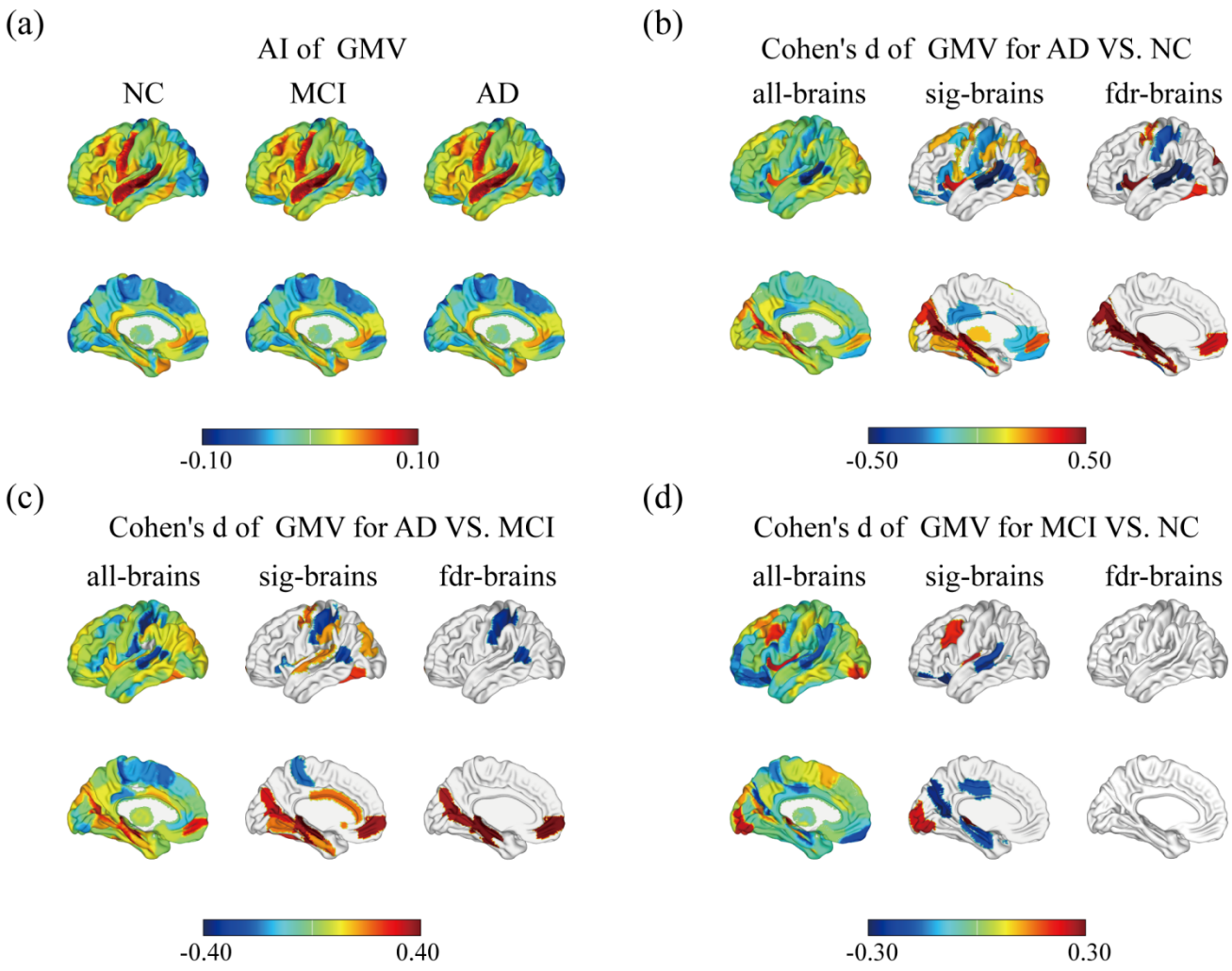

Supplementary Figure 1. Original asymmetry index and brain regions of group difference with significant lateralization in GMV. (a) AI of GMV among AD, MCI and NC. The results are projected onto homologous region pairs in a hemispheric view (left hemisphere illustrated as an example). Values on brain regions represent AI of GMV for each group. Larger AI reflecting greater leftward with warmer color. (b) The significant effect brain map of group difference in AD and NC with all brains, significant brains ($p < 0.05$) and significant brains after FDR correction (p-FDR < 0.05). (c) The significant effect brain map of group difference in AD and MCI with all brains, significant brains ($p < 0.05$) and significant brains after FDR correction (p-FDR < 0.05). (d) The significant effect brain map of group difference in MCI and NC with all brains, significant brains ($p < 0.05$) and significant brains after FDR correction (p-FDR < 0.05). Regions with statistically significant difference are highlighted, while gray areas denote non-significant regions. The color bar denotes positive Cohen's d effect size (warm tones: AD exhibits leftward AI) and negative Cohen's d effect size (cool tones: AD exhibits rightward AI).

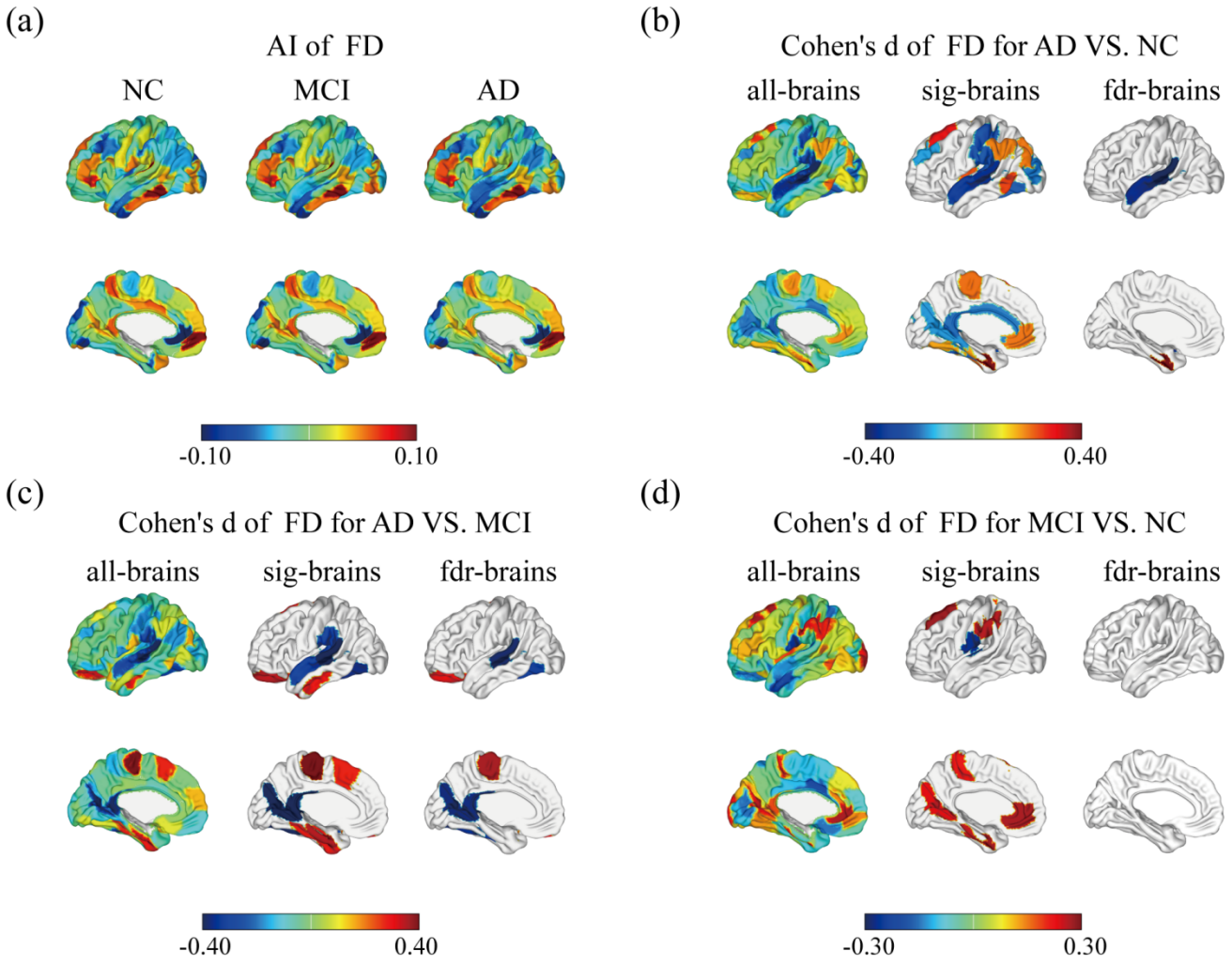

Supplementary Figure 2. Original asymmetry index and brain regions of group difference with significant lateralization in FD. (a) AI of FD among AD, MCI and NC. The results are projected onto homologous region pairs in a hemispheric view (left hemisphere illustrated as an example). Values on brain regions represent AI of FD for each group. Larger AI reflecting greater leftward with warmer color. (b) The significant effect brain map of group difference in AD and NC with all brains, significant brains ($p < 0.05$) and significant brains after FDR correction (p-FDR < 0.05). (c) The significant effect brain map of group difference in AD and MCI with all brains, significant brains ($p < 0.05$) and significant brains after FDR correction (p-FDR < 0.05). (d) The significant effect brain map of group difference in MCI and NC with all brains, significant brains ($p < 0.05$) and significant brains after FDR correction (p-FDR < 0.05). Regions with statistically significant difference are highlighted, while gray areas denote non-significant regions. The color bar denotes positive Cohen's d effect size (warm tones: AD exhibits leftward AI) and negative Cohen's d effect size (cool tones: AD exhibits rightward AI).

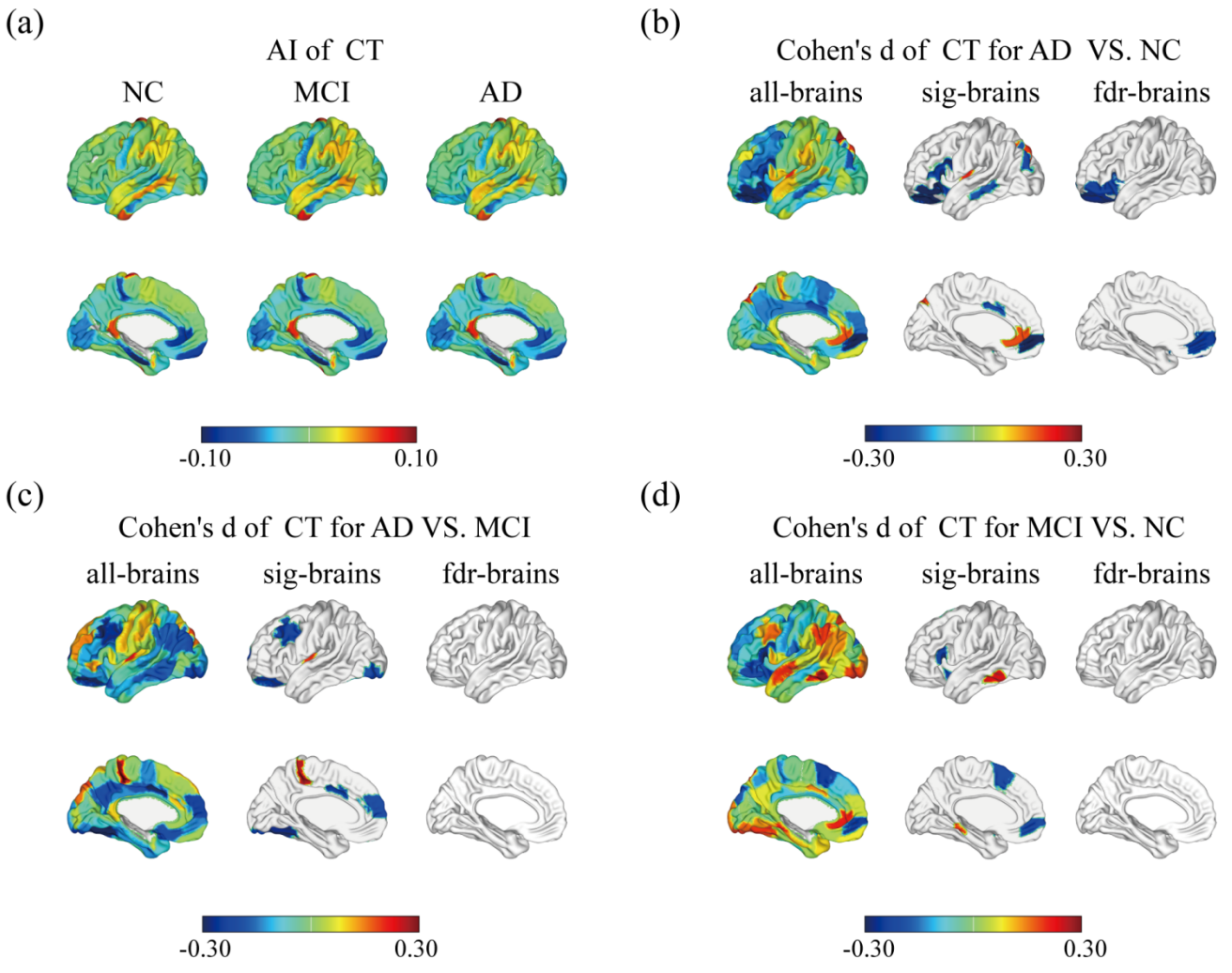

Supplementary Figure 3. Original asymmetry index and brain regions of group difference with significant lateralization in CT. (a) AI of CT among AD, MCI and NC. The results are projected onto homologous region pairs in a hemispheric view (left hemisphere illustrated as an example). Values on brain regions represent AI of CT for each group. Larger AI reflecting greater leftward with warmer color. (b) The significant effect brain map of group difference in AD and NC with all brains, significant brains ($p < 0.05$) and significant brains after FDR correction (p-FDR < 0.05). (c) The significant effect brain map of group difference in AD and MCI with all brains,

significant brains ($p < 0.05$) and significant brains after FDR correction (p-FDR < 0.05). (d) The significant effect brain map of group difference in MCI and NC with all brains, significant brains ($p < 0.05$) and significant brains after FDR correction (p-FDR < 0.05). Regions with statistically significant difference are highlighted, while gray areas denote non-significant regions. The color bar denotes positive Cohen's d effect size (warm tones: AD exhibits leftward AI) and negative Cohen's d effect size (cool tones: AD exhibits rightward AI).

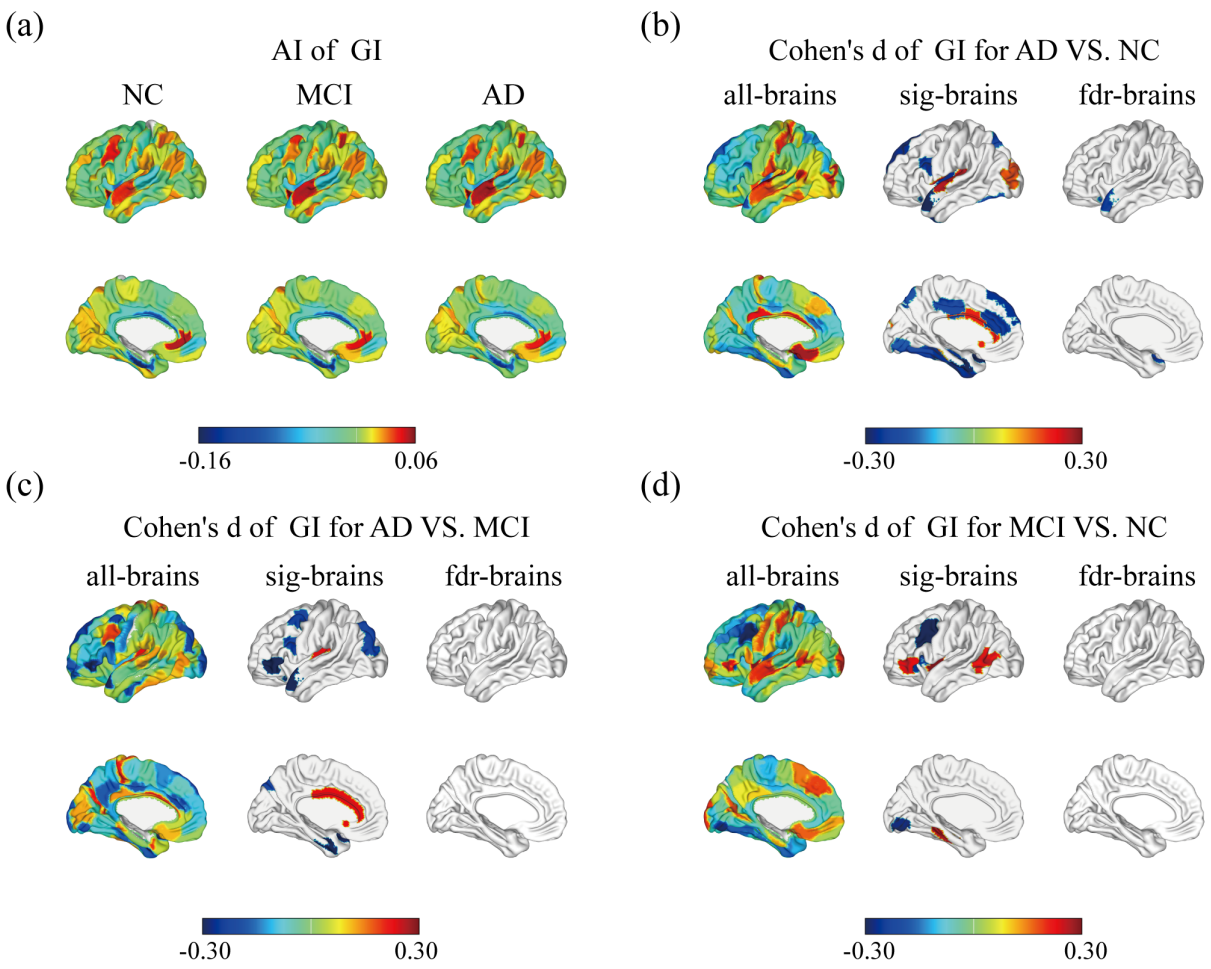

Supplementary Figure 4. Original asymmetry index and brain regions of group difference with significant lateralization in GI. (a) AI of GI among AD, MCI and NC. The results are projected onto homologous region pairs in a hemispheric view (left hemisphere illustrated as an example). Values on brain regions represent AI of GI for each group. Larger AI reflecting greater leftward with warmer color. (b) The significant effect brain map of group difference in AD and NC with all brains, significant brains ($p < 0.05$) and significant brains after FDR correction (p-FDR < 0.05). (c) The significant effect brain map of group difference in AD and MCI with all brains, significant brains ($p < 0.05$) and significant brains after FDR correction (p-FDR < 0.05). (d) The significant effect brain map of group difference in MCI and NC with all brains, significant brains ($p < 0.05$) and significant brains after FDR correction (p-FDR < 0.05). Regions with statistically significant difference are highlighted, while gray areas denote non-significant regions. The color bar denotes positive Cohen's d effect size (warm tones: AD exhibits leftward AI) and negative Cohen's d effect size (cool tones: AD exhibits rightward AI).

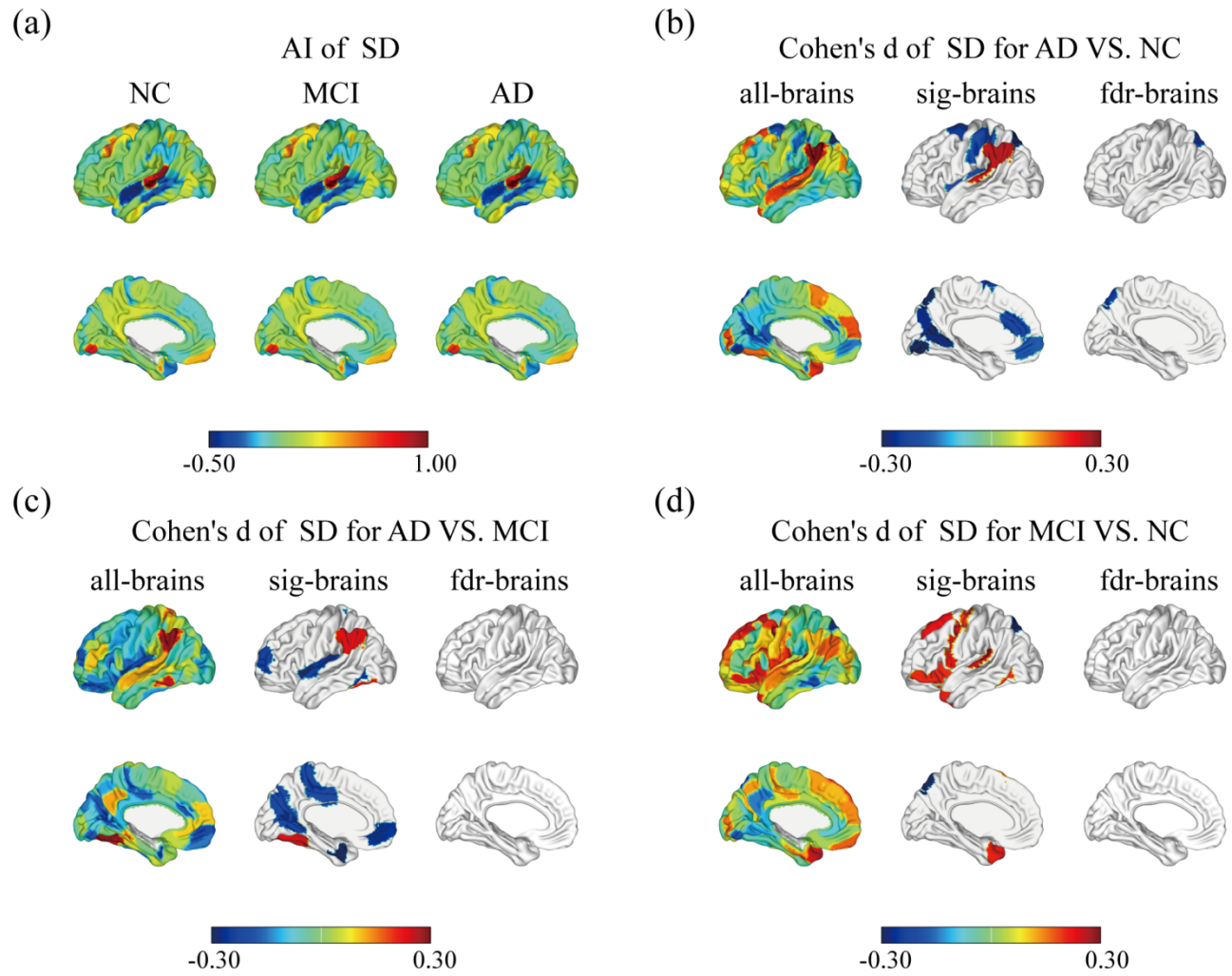

Supplementary Figure 5. Original asymmetry index and brain regions of group difference with significant lateralization in SD. (a) AI of SD among AD, MCI and NC. The results are projected onto homologous region pairs in a hemispheric view (left hemisphere illustrated as an example). Values on brain regions represent AI of SD for each group. Larger AI reflecting greater leftward with warmer

color. (b) The significant effect brain map of group difference in AD and NC with all brains, significant brains ($p < 0.05$) and significant brains after FDR correction (p-FDR < 0.05). (c) The significant effect brain map of group difference in AD and MCI with all brains, significant brains ($p < 0.05$) and significant brains after FDR correction (p-FDR < 0.05). (d) The significant effect brain map of group difference in MCI and NC with all brains, significant brains ($p < 0.05$) and significant brains after FDR correction (p-FDR < 0.05). Regions with statistically significant difference are highlighted, while gray areas denote non-significant regions. The color bar denotes positive Cohen's d effect size (warm tones: AD exhibits leftward AI) and negative Cohen's d effect size (cool tones: AD exhibits rightward AI).

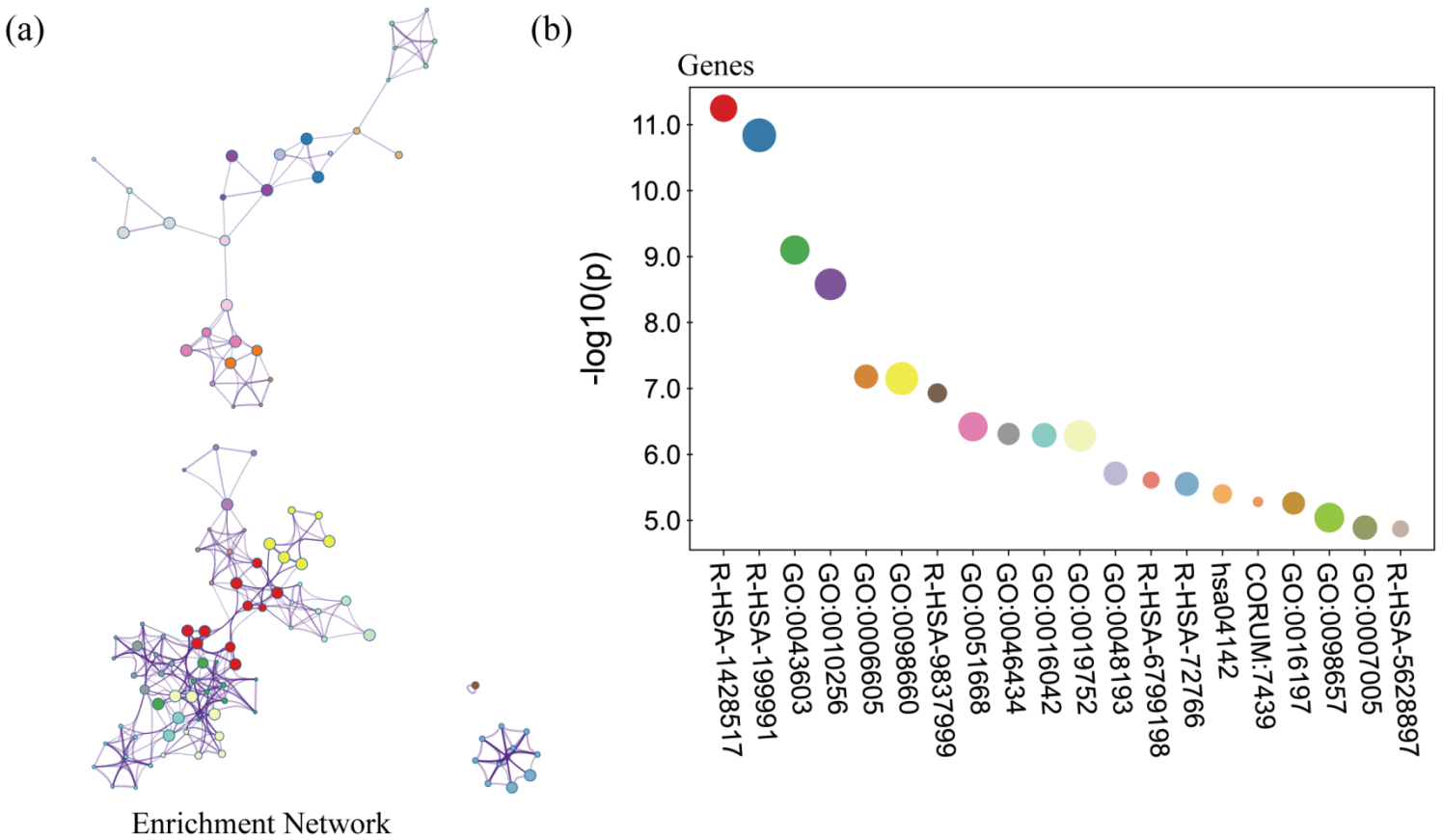

Supplementary Figure 6. Gene analysis results for group difference pattern of HFC between AD and MCI. (a) Gene enrichment network for strength pattern of HFC. (b) Top 20 clusters with their representative enriched terms (one per cluster). The circle size represents the number of genes involved in the specific term.

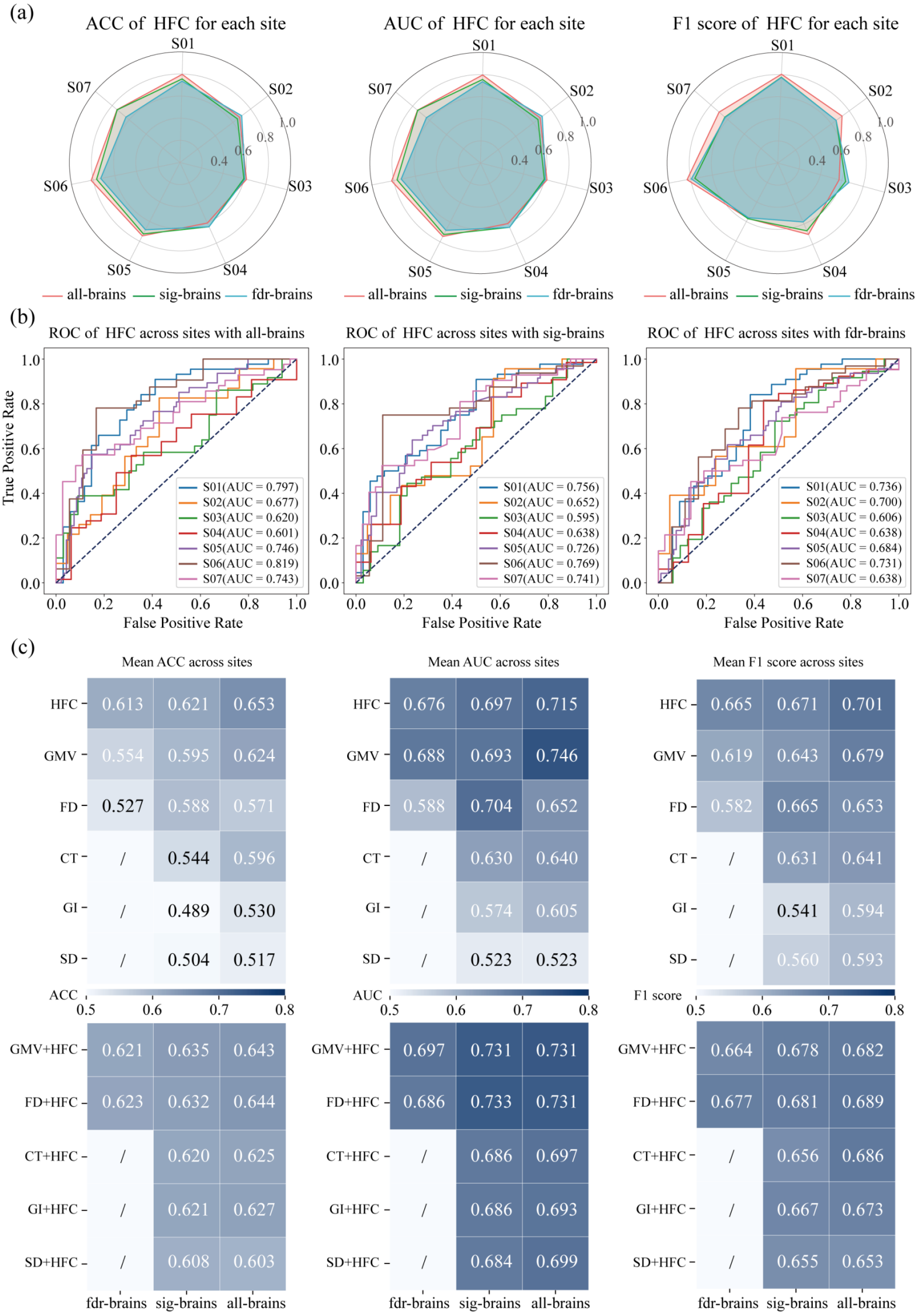

Supplementary Figure 7. Model performance under different feature selection schemes in classification task distinguishing AD from MCI. (a) Classification performance (ACC, AUC, and F1 score for each site). (b) ROC curve of the model with the features used the HFC across all brains, significant brains (sig-brains) and significant brains after FDR correction (FDR-brains). (c) Classification performance (site averaged ACC, AUC, and F1 score) across varying feature dimensions (x-axis) and metric combinations (y-axis). Empty cells (marked with "/") indicate no features selected under the corresponding metric. Darker hues in the color bar denote superior model performance in ACC, AUC and F1 score.

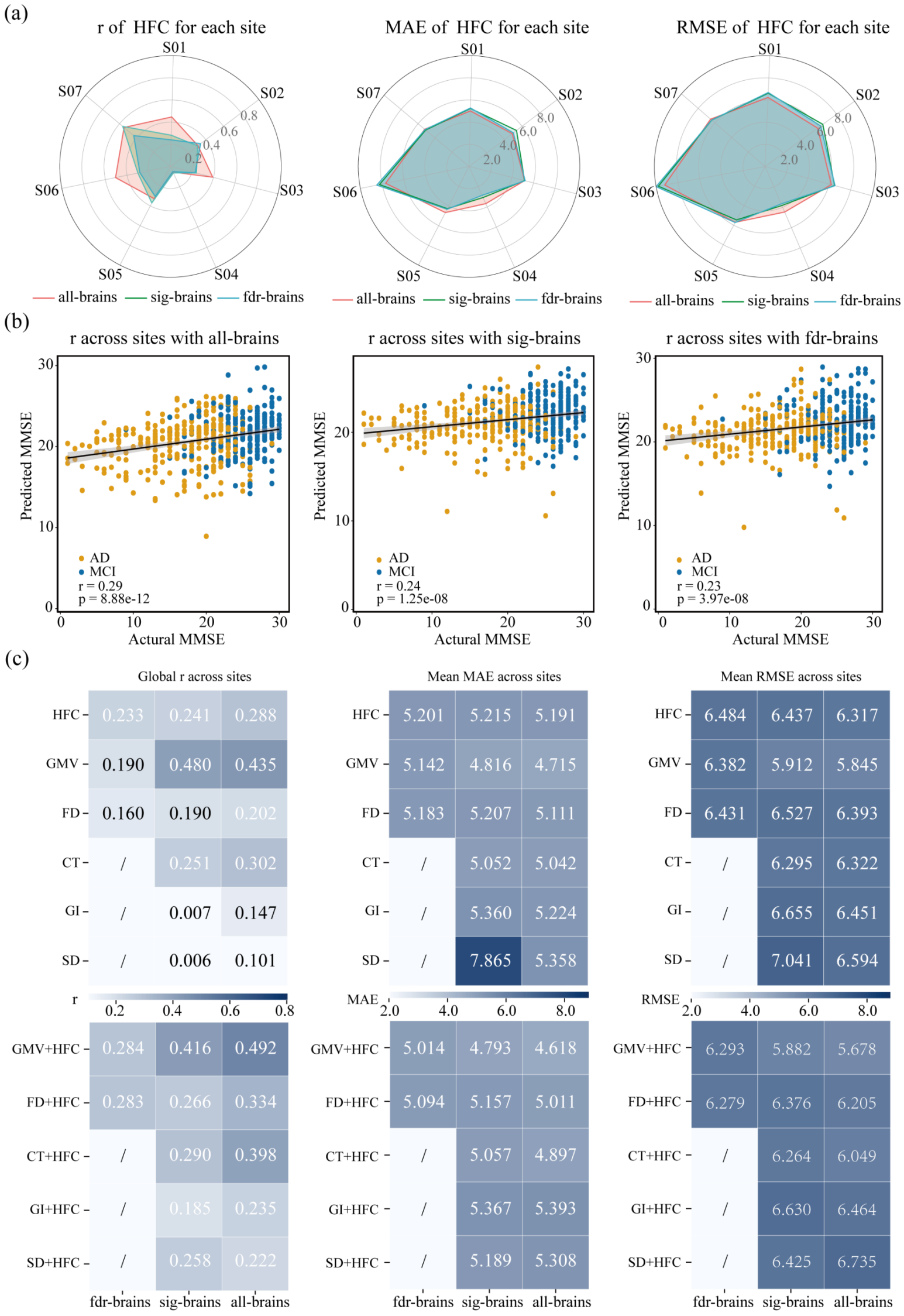

Supplementary Figure 8. Model performance under different feature selection schemes based on differences between AD and MCI in prediction of the clinical cognitive scores. (a) Prediction performance (r, MAE, and RMSE for each site). (b) Scatter plot of the model with the features used the HFC across all brains, significant brains (sig-brains) and significant brains after FDR correction (FDR-brains). (c) Prediction performance (site averaged r, MAE, and RMSE) across varying feature dimensions (x-axis) and metric combinations (y-axis). Empty cells (marked with "/") indicate no features selected under the corresponding metric. Darker hues in the color bar denote superior model performance in r while worse model performance in MAE and RMSE.

Supplementary Tables

Supplementary Table S1. Brain regions of group difference with significant lateralization in GMV after FDR correction.

GMV			NC	MCI	AD	AD VS. NC		AD VS. MCI	
Lobe	Gyrus	Region	Mean AI	Mean AI	Mean AI	Cohen's d	p-FDR	Cohen's d	p-FDR
Frontal Lobe	IFG	A44op	0.039	0.026	-0.004	-0.359	<0.001	-	-
	OrG	A14m	-0.307	-0.308	-0.274	0.321	0.003	0.411	0.011
	PrG	A6cdl	-0.331	-0.331	-0.299	0.247	0.037	-	-
Temporal Lobe	STG	A22c	0.867	0.833	0.770	-0.548	0.003	-	-
	ITG	A20iv	0.889	0.868	0.847	-0.243	0.041	-	-
	FuG	A37lv	0.008	0.000	0.048	0.272	0.027	-	-
	PhG	A35_36r	-0.017	0.009	0.069	0.372	0.004	-	-
		A35_36c	-0.153	-0.149	-0.088	0.501	<0.001	0.486	0.002
		TH	-0.069	-0.067	-0.013	0.413	<0.001	0.402	0.021
Parietal Lobe	pSTS	cpSTS	0.237	0.221	0.179	-0.361	0.050	-0.287	0.021
	PoG	A2	0.091	0.097	0.056	-0.237	0.047	-0.336	0.005
Insular Lobe	INS	dIa	0.180	0.214	0.228	0.469	<0.001	-	-
		dId	0.167	0.195	0.209	0.427	<0.001	-	-
Occipital Lobe	MVOcC	vmPOS	-0.196	-0.173	-0.138	0.525	<0.001	0.362	0.010
	LOcC	msOccG	-0.235	-0.189	-0.190	0.369	<0.001	-	-
Subcortical Nuclei	Hipp	cHipp	-0.101	-0.087	-0.029	0.720	<0.001	0.560	0.002
	Tha	PPtha	0.246	0.275	0.300	0.438	0.027	-	-
		Otha	0.157	0.214	0.231	0.428	0.003	-	-

"Lobe" is the major lobe of the brain. "Gyrus" is the specific gyrus within the lobe. "Number" is the identifier for the brain region. "Mean AI" (NC, MCI, AD) means the average asymmetry index for each group. The effect size (Cohen's d) and the False Discovery Rate-adjusted p-FDR value for the comparison between groups. A dash (-) in the statistical columns indicates that the data is not applicable or not reported for that specific comparison.

Supplementary Table S2. Brain regions of group difference with significant lateralization in FD after FDR correction.

FD			NC	MCI	AD	AD VS. NC		AD VS. MCI	
Lobe	Gyrus	Region	Mean AI	Mean AI	Mean AI	Cohen's d	p-FDR	Cohen's d	p-FDR
Frontal Lobe	OrG	A11l	-0.015	-0.018	-0.009	-	-	0.292	0.040
	PCL	A4ll	-0.037	-0.041	-0.023	-	-	0.359	0.005
Temporal Lobe	STG	A22c	0.009	-0.007	-0.033	-0.394	0.032	-0.381	0.047
		A22r	-0.014	-0.033	-0.046	-0.355	0.022	-	-
	FuG	A37lv	-0.033	-0.028	-0.056	-	-	-0.322	0.013
	PhG	A35_36r	-0.093	-0.074	-0.049	0.526	<0.001	-	-
Limbic Lobe	CG	A23v	0.060	0.059	0.045	-	-	-0.369	0.018
Occipital Lobe	MVOcC	vmPOS	0.048	0.052	0.034	-	-	-0.370	0.018

"Lobe" is the major lobe of the brain. "Gyrus" is the specific gyrus within the lobe. "Number" is the identifier for the brain region. "Mean AI" (NC, MCI, AD) means the average asymmetry index for each group. The effect size (Cohen's d) and the False Discovery Rate-adjusted p-FDR value for the comparison between groups. A dash (-) in the statistical columns indicates that the data is not applicable or not reported for that specific comparison.

Supplementary Table S3. Brain regions of group difference with significant lateralization in CT after FDR correction.

CT			NC	MCI	AD	AD VS. NC	
Lobe	Gyrus	Region	Mean AI	Mean AI	Mean AI	Cohen's d	p-FDR
Frontal Lobe	IFG	A44op	-0.016	-0.022	-0.028	-0.299	0.022
	OrG	A14m	0.002	-0.014	-0.021	-0.326	0.020
		A11l	-0.019	-0.022	-0.039	-0.360	0.013
		A12_47l	0.008	0.002	-0.010	-0.298	0.039

"Lobe" is the major lobe of the brain. "Gyrus" is the specific gyrus within the lobe. "Number" is the identifier for the brain region. "Mean AI" (NC, MCI, AD) means the average asymmetry index for each group. The effect size (Cohen's d) and the False Discovery Rate-adjusted (p-FDR) value for the comparison between groups. A dash (-) in the statistical columns indicates that the data is not applicable or not reported for that specific comparison.

Supplementary Table S4. Brain regions of group difference with significant lateralization in GI after FDR correction.

GI			NC	MCI	AD	AD VS. NC	
Lobe	Gyrus	Region	Mean AI	Mean AI	Mean AI	Cohen's d	p-FDR
Temporal Lobe	STG	A38l	-0.063	-0.063	-0.087	-0.320	0.026

"Lobe" is the major lobe of the brain. "Gyrus" is the specific gyrus within the lobe. "Number" is the identifier for the brain region. "Mean AI" (NC, MCI, AD) means the average asymmetry index for each group. The effect size (Cohen's d) and the False Discovery Rate-adjusted

p-FDR value for the comparison between groups. A dash (-) in the statistical columns indicates that the data is not applicable or not reported for that specific comparison.

Supplementary Table S5. Brain regions of group difference with significant lateralization in SD after FDR correction.

SD			NC	MCI	AD	AD VS. NC	
Lobe	Gyrus	Region	Mean AI	Mean AI	Mean AI	Cohen's d	p-FDR
Parietal Lobe	SPL	A7c	0.181	0.116	0.118	-0.331	0.016

"Lobe" is the major lobe of the brain. "Gyrus" is the specific gyrus within the lobe. "Number" is the identifier for the brain region. "Mean AI" (NC, MCI, AD) means the average asymmetry index for each group. The effect size (Cohen's d) and the False Discovery Rate-adjusted p-FDR value for the comparison between groups. A dash (-) in the statistical columns indicates that the data is not applicable or not reported for that specific comparison.

Supplementary Table S6. Detailed statistical results of gene expression for AD VS. NC.

GO	Category	Description	Count	%	Log10(P)	Log10(q)
R-HSA-8953854	Reactome Gene Sets	Metabolism of RNA	81	8.19	-24.74	-20.58
R-HSA-1428517	Reactome Gene Sets	Aerobic respiration and respiratory electron transport	43	4.35	-18.42	-14.68
GO:0007005	GO Biological Processes	mitochondrion organization	53	5.36	-17.7	-14.06
GO:0033365	GO Biological Processes	protein localization to organelle	76	7.68	-16.22	-12.95
GO:0022613	GO Biological Processes	ribonucleoprotein complex biogenesis	53	5.36	-13.81	-10.85
GO:1903320	GO Biological Processes	regulation of protein modification by small protein conjugation or removal	35	3.54	-12.66	-9.89
hsa05022	KEGG Pathway	Pathways of neurodegeneration - multiple diseases	50	5.06	-12.09	-9.38
GO:0072655	GO Biological Processes	establishment of protein localization to mitochondrion	19	1.92	-11.38	-8.76
GO:0010506	GO Biological Processes	regulation of autophagy	41	4.15	-11.38	-8.76
GO:0006914	GO Biological Processes	autophagy	39	3.94	-11.27	-8.67
GO:0030163	GO Biological Processes	protein catabolic process	65	6.57	-11.05	-8.47
R-HSA-1632852	Reactome Gene Sets	Macroautophagy	22	2.22	-10.24	-7.77
GO:0051604	GO Biological Processes	protein maturation	50	5.06	-10.21	-7.74
R-HSA-8951664	Reactome Gene Sets	Neddylation	28	2.83	-10.06	-7.62
GO:0016050	GO Biological Processes	vesicle organization	38	3.84	-9.91	-7.47
R-HSA-5368286	Reactome Gene Sets	Mitochondrial translation initiation	18	1.82	-9.54	-7.14
GO:0034655	GO Biological Processes	nucleobase-containing compound catabolic process	34	3.44	-8.28	-6
GO:0042273	GO Biological Processes	ribosomal large subunit biogenesis	14	1.42	-7.73	-5.49
R-HSA-199991	Reactome Gene Sets	Membrane Trafficking	45	4.55	-7.62	-5.39
GO:0022411	GO Biological Processes	cellular component disassembly	31	3.13	-7.56	-5.34

Top 20 clusters with their representative enriched terms (one per cluster). "Count" is the number of genes in the user-provided lists with membership in the given ontology term. "Gene proportion (%)" is the percentage of all of the user-provided genes that are found in the given ontology term (only input genes with at least one ontology term annotation are included in the calculation). "Log10(P)" is the p-value in log base 10. "Log10(q)" is the multi-test adjusted p-value in log base 10.

Supplementary Table S7. Detailed statistical results of gene expression for AD VS. MCI.

GO	Category	Description	Count	%	Log10(P)	Log10(q)
R-HSA-1428517	Reactome Gene Sets	Aerobic respiration and respiratory electron transport	25	4.73	-11.25	-6.91
R-HSA-199991	Reactome Gene Sets	Membrane Trafficking	39	7.39	-10.84	-6.79
GO:0043603	GO Biological Processes	amide metabolic process	29	5.49	-9.1	-5.36
GO:0010256	GO Biological Processes	endomembrane system organization	34	6.44	-8.58	-5.01
GO:0006605	GO Biological Processes	protein targeting	19	3.6	-7.18	-3.71
GO:0098660	GO Biological Processes	inorganic ion transmembrane transport	37	7.01	-7.15	-3.71
R-HSA-9837999	Reactome Gene Sets	Mitochondrial protein degradation	12	2.27	-6.93	-3.59
GO:0051668	GO Biological Processes	localization within membrane	29	5.49	-6.42	-3.22
GO:0046434	GO Biological Processes	organophosphate catabolic process	16	3.03	-6.31	-3.16
GO:0016042	GO Biological Processes	lipid catabolic process	20	3.79	-6.29	-3.16
GO:0019752	GO Biological Processes	carboxylic acid metabolic process	35	6.63	-6.28	-3.16
GO:0048193	GO Biological Processes	Golgi vesicle transport	19	3.6	-5.71	-2.79
R-HSA-6799198	Reactome Gene Sets	Complex I biogenesis	9	1.7	-5.61	-2.7
R-HSA-72766	Reactome Gene Sets	Translation	19	3.6	-5.55	-2.67
hsa04142	KEGG Pathway	Lysosome	12	2.27	-5.4	-2.54
CORUM:7439	CORUM	ECT2-KIF23-RACGAP1 complex	3	0.57	-5.28	-2.47
GO:0016197	GO Biological Processes	endosomal transport	17	3.22	-5.26	-2.47
GO:0098657	GO Biological Processes	import into cell	30	5.68	-5.04	-2.3
GO:0007005	GO Biological Processes	mitochondrion organization	20	3.79	-4.89	-2.22
R-HSA-5628897	Reactome Gene Sets	TP53 Regulates Metabolic Genes	9	1.7	-4.87	-2.22

Supplementary Table S8. The statistical results of the classification between AD and NC for each site.

	Features across all-brains			Features across sig-brains			Features across with FDR-brains		
Site	ACC	AUC	F1 score	ACC	AUC	F1 score	ACC	AUC	F1 score
S01	0.833	0.926	0.857	0.833	0.899	0.841	0.774	0.853	0.800
S02	0.841	0.896	0.844	0.750	0.884	0.792	0.841	0.920	0.857
S03	0.700	0.775	0.763	0.683	0.751	0.740	0.700	0.753	0.769
S04	0.561	0.607	0.657	0.589	0.616	0.645	0.495	0.573	0.591
S05	0.779	0.814	0.747	0.699	0.787	0.653	0.717	0.782	0.667
S06	0.736	0.856	0.788	0.774	0.859	0.800	0.755	0.860	0.787
S07	0.765	0.832	0.762	0.765	0.820	0.737	0.788	0.819	0.757

"ACC" is the classification Accuracy achieved on the respective site. "AUC" means the Area Under the ROC Curve, which measures the model's ability to distinguish between classes across all classification thresholds. The F1 score, which is the harmonic mean of precision and recall.

Supplementary Table S9. The statistical results of the classification between AD and MCI for each site.

	Features across all-brains			Features across sig-brains			Features across with FDR-brains		
Site	ACC	AUC	F1 score	ACC	AUC	F1 score	ACC	AUC	F1 score
S01	0.744	0.797	0.804	0.705	0.756	0.777	0.731	0.736	0.774
S02	0.682	0.677	0.720	0.591	0.652	0.654	0.591	0.700	0.654
S03	0.507	0.620	0.575	0.536	0.595	0.636	0.580	0.606	0.667
S04	0.593	0.601	0.703	0.568	0.638	0.667	0.481	0.638	0.580
S05	0.603	0.746	0.569	0.617	0.726	0.571	0.589	0.684	0.561
S06	0.800	0.819	0.833	0.700	0.769	0.762	0.740	0.731	0.794
S07	0.646	0.743	0.702	0.633	0.741	0.633	0.582	0.638	0.629

Supplementary Table S10. The statistical results of the prediction between AD and NC for each site.

	Features across all-brains				Features across sig-brains				Features across with FDR-brains			
Site	MAE	RMSE	r	p	MAE	RMSE	r	p	MAE	RMSE	r	p
S01	4.258	5.899	0.616	<0.001	4.660	5.985	0.588	<0.001	5.153	6.517	0.471	<0.001
S02	4.183	5.348	0.589	<0.001	4.666	6.197	0.574	<0.001	4.109	5.525	0.591	<0.001
S03	5.617	6.749	0.549	<0.001	5.775	7.043	0.505	<0.001	6.002	7.343	0.385	0.002
S04	4.572	5.375	0.218	0.024	4.551	5.431	0.179	0.064	4.818	5.734	0.104	0.289
S05	5.165	6.644	0.415	<0.001	4.995	6.727	0.426	<0.001	5.234	6.892	0.391	<0.001
S06	7.539	9.425	0.650	<0.001	7.425	9.452	0.661	<0.001	7.714	9.914	0.630	<0.001
S07	4.913	6.257	0.626	<0.001	4.922	6.382	0.598	<0.001	5.320	7.004	0.552	<0.001

MAE, Mean Absolute Error. RMSE, Root Mean Square Error. r, The correlation coefficient. p, The p-value.

Supplementary Table S11. The statistical results of the prediction between AD and MCI for each site.

	Features across all-brains				Features across sig-brains				Features across with FDR-brains			
Site	MAE	RMSE	r	p	MAE	RMSE	r	p	MAE	RMSE	r	p
S01	5.011	6.238	0.447	<0.001	5.237	6.624	0.282	0.013	5.279	6.688	0.240	0.034
S02	4.895	5.876	0.311	0.040	5.378	6.453	0.307	0.043	5.024	6.209	0.341	0.023
S03	5.178	6.198	0.393	<0.001	5.177	6.502	0.242	0.045	5.228	6.545	0.230	0.058
S04	3.681	4.469	0.056	0.622	3.076	3.830	0.064	0.571	2.861	3.672	0.051	0.656
S05	4.675	5.705	0.326	<0.001	4.284	5.466	0.370	<0.001	4.345	5.731	0.304	<0.001
S06	7.676	9.213	0.506	<0.001	8.245	9.794	0.300	0.034	8.493	10.166	0.282	0.047
S07	5.224	6.517	0.547	<0.001	5.108	6.387	0.562	<0.001	5.175	6.394	0.433	<0.001

Supplementary Table S12. Brainnetome atlas.

The human Brainnetome Atlas was employed. The atlas was derived from a parcellation approach based on connectivity information and has been used in brain network studies. The atlas consists of 246 subregions in the cerebrum (210 cortical and 36 subcortical regions) (http://atlas.brainnetome.org). Before we extracted the mean regional time series, any voxel with an amplitude value less than 0.05 and any area where there was no fMRI signal recorded from one or more participants was excluded from the study. This resulted in a set of 246 regional areas of the Brainnetome Atlas being included for further analysis. The detailed information of 246 regions was listed as follows.

Lobe	Gyrus	Left and Right Hemisphere	Label ID.L	Label ID.R	Anatomical and modified Cyto-architectonic descriptions	lh.MNI(X,Y,Z)	rh.MNI(X,Y,Z)
Frontal Lobe	SFG, Superior Frontal Gyrus	SFG_L(R)_7_1	1	2	A8m, medial area 8	-5 ,15, 54	7, 16, 54
		SFG_L(R)_7_2	3	4	A8dl, dorsolateral area 8	-18, 24, 53	22, 26, 51
		SFG_L(R)_7_3	5	6	A9l, lateral area 9	-11, 49, 40	13, 48, 40
		SFG_L(R)_7_4	7	8	A6dl, dorsolateral area 6	-18, -1, 65	20, 4, 64
		SFG_L(R)_7_5	9	10	A6m, medial area 6	-6, -5, 58	7, -4, 60
		SFG_L(R)_7_6	11	12	A9m, medial area 9	-5, 36, 38	6, 38, 35
		SFG_L(R)_7_7	13	14	A10m, medial area 10	-8, 56, 15	8, 58, 13
	MFG, Middle Frontal Gyrus	MFG_L(R)_7_1	15	16	A9/46d, dorsal area 9/46	-27, 43, 31	30, 37, 36
		MFG_L(R)_7_2	17	18	IFJ, inferior frontal junction	-42, 13, 36	42, 11, 39
		MFG_L(R)_7_3	19	20	A46, area 46	-28, 56, 12	28, 55, 17
		MFG_L(R)_7_4	21	22	A9/46v, ventral area 9/46	-41, 41, 16	42, 44, 14
		MFG_L(R)_7_5	23	24	A8vl, ventrolateral area 8	-33, 23, 45	42, 27, 39
		MFG_L(R)_7_6	25	26	A6vl, ventrolateral area 6	-32, 4, 55	34, 8, 54
		MFG_L(R)_7_7	27	28	A10l, lateral area10	-26, 60, -6	25, 61, -4
	IFG, Inferior Frontal Gyrus	IFG_L(R)_6_1	29	30	A44d, dorsal area 44	-46, 13, 24	45, 16, 25
		IFG_L(R)_6_2	31	32	IFS, inferior frontal sulcus	-47, 32, 14	48, 35, 13
		IFG_L(R)_6_3	33	34	A45c, caudal area 45	-53, 23, 11	54, 24, 12
		IFG_L(R)_6_4	35	36	A45r, rostral area 45	-49, 36, -3	51, 36, -1
		IFG_L(R)_6_5	37	38	A44op, opercular area 44	-39, 23, 4	42, 22, 3
		IFG_L(R)_6_6	39	40	A44v, ventral area 44	-52, 13, 6	54, 14, 11
	OrG, Orbital Gyrus	OrG_L(R)_6_1	41	42	A14m, medial area 14	-7, 54, -7	6, 47, -7
		OrG_L(R)_6_2	43	44	A12/47o, orbital area 12/47	-36, 33, -16	40, 39, -14
		OrG_L(R)_6_3	45	46	A11l, lateral area 11	-23, 38, -18	23, 36, -18
		OrG_L(R)_6_4	47	48	A11m, medial area 11	-6, 52, -19	6, 57, -16
		OrG_L(R)_6_5	49	50	A13, area 13	-10, 18, -19	9, 20, -19
		OrG_L(R)_6_6	51	52	A12/47l, lateral area 12/47	-41, 32, -9	42, 31, -9
	PrG, Precentral Gyrus	PrG_L(R)_6_1	53	54	A4hf, area 4(head and face region)	-49, -8, 39	55, -2, 33
		PrG_L(R)_6_2	55	56	A6cdl, caudal dorsolateral area 6	-32, -9, 58	33, -7, 57
		PrG_L(R)_6_3	57	58	A4ul, area 4(upper limb region)	-26, -25, 63	34, -19, 59
		PrG_L(R)_6_4	59	60	A4t, area 4(trunk region)	-13, -20, 73	15, -22, 71
		PrG_L(R)_6_5	61	62	A4tl, area 4(tongue and larynx region)	-52, 0, 8	54, 4, 9
		PrG_L(R)_6_6	63	64	A6cvl, caudal ventrolateral area 6	-49, 5, 30	51, 7, 30
	PCL, Paracentral Lobule	PCL_L(R)_2_1	65	66	A1/2/3ll, area1/2/3 (lower limb region)	-8, -38, 58	10, -34, 54
		PCL_L(R)_2_2	67	68	A4ll, area 4, (lower limb region)	-4, -23, 61	5, -21, 61
Temporal Lobe	STG, Superior Temporal Gyrus	STG_L(R)_6_1	69	70	A38m, medial area 38	-32, 14, -34	31, 15, -34
		STG_L(R)_6_2	71	72	A41/42, area 41/42	-54, -32, 12	54, -24, 11
		STG_L(R)_6_3	73	74	TE1.0 and TE1.2	-50, -11, 1	51, -4, -1
		STG_L(R)_6_4	75	76	A22c, caudal area 22	-62, -33, 7	66, -20, 6

		STG_L(R)_6_5	77	78	A38l, lateral area 38	-45, 11, -20	47, 12, -20
		STG_L(R)_6_6	79	80	A22r, rostral area 22	-55, -3, -10	56, -12, -5
	MTG, Middle Temporal Gyrus	MTG_L(R)_4_1	81	82	A21c, caudal area 21	-65, -30, -12	65, -29, -13
		MTG_L(R)_4_2	83	84	A21r, rostral area 21	-53, 2, -30	51, 6, -32
		MTG_L(R)_4_3	85	86	A37dl, dorsolateral area37	-59, -58, 4	60, -53, 3
		MTG_L(R)_4_4	87	88	aSTS, anterior superior temporal sulcus	-58, -20, -9	58, -16, -10
	ITG, Inferior Temporal Gyrus	ITG_L(R)_7_1	89	90	A20iv, intermediate ventral area 20	-45, -26, -27	46, -14, -33
		ITG_L(R)_7_2	91	92	A37elv, extreme lateroventral area37	-51, -57, -15	53, -52, -18
		ITG_L(R)_7_3	93	94	A20r, rostral area 20	-43, -2, -41	40, 0, -43
		ITG_L(R)_7_4	95	96	A20il, intermediate lateral area 20	-56, -16, -28	55, -11, -32
		ITG_L(R)_7_5	97	98	A37vl, ventrolateral area 37	-55, -60, -6	54, -57, -8
		ITG_L(R)_7_6	99	100	A20cl, caudolateral of area 20	-59, -42, -16	61, -40, -17
		ITG_L(R)_7_7	101	102	A20cv, caudoventral of area 20	-55, -31, -27	54, -31, -26
	FuG, Fusiform Gyrus	FuG_L(R)_3_1	103	104	A20rv, rostroventral area 20	-33, -16, -32	33, -15, -34
		FuG_L(R)_3_2	105	106	A37mv, medioventral area37	-31, -64, -14	31, -62, -14
		FuG_L(R)_3_3	107	108	A37lv, lateroventral area37	-42, -51, -17	43, -49, -19
	PhG, Parahippocampal Gyrus	PhG_L(R)_6_1	109	110	A35/36r, rostral area 35/36	-27, -7, -34	28, -8, -33
		PhG_L(R)_6_2	111	112	A35/36c, caudal area 35/36	-25, -25, -26	26, -23, -27
		PhG_L(R)_6_3	113	114	TL, area TL (lateral PPHC, posterior parahippocampal gyrus)	-28, -32, -18	30, -30, -18
		PhG_L(R)_6_4	115	116	A28/34, area 28/34 (EC, entorhinal cortex)	-19, -12, -30	19, -10, -30
		PhG_L(R)_6_5	117	118	TI, area TI(temporal agranular insular cortex)	-23, 2, -32	22, 1, -36
		PhG_L(R)_6_6	119	120	TH, area TH (medial PPHC)	-17, -39, -10	19, -36, -11
	pSTS, posterior Superior Temporal Sulcus	pSTS_L(R)_2_1	121	122	rpSTS, rostroposterior superior temporal sulcus	-54, -40, 4	53, -37, 3
		pSTS_L(R)_2_2	123	124	cpSTS, caudoposterior superior temporal sulcus	-52, -50, 11	57, -40, 12
Parietal Lobe	SPL, Superior Parietal Lobule	SPL_L(R)_5_1	125	126	A7r, rostral area 7	-16, -60, 63	19, -57, 65
		SPL_L(R)_5_2	127	128	A7c, caudal area 7	-15, -71, 52	19, -69, 54
		SPL_L(R)_5_3	129	130	A5l, lateral area 5	-33, -47, 50	35, -42, 54
		SPL_L(R)_5_4	131	132	A7pc, postcentral area 7	-22, -47, 65	23, -43, 67
		SPL_L(R)_5_5	133	134	A7ip, intraparietal area 7(hIP3)	-27, -59, 54	31, -54, 53
	IPL, Inferior Parietal Lobule	IPL_L(R)_6_1	135	136	A39c, caudal area 39(PGp)	-34, -80, 29	45, -71, 20
		IPL_L(R)_6_2	137	138	A39rd, rostrodorsal area 39(Hip3)	-38, -61, 46	39, -65, 44
		IPL_L(R)_6_3	139	140	A40rd, rostrodorsal area 40(PFt)	-51, -33, 42	47, -35, 45
		IPL_L(R)_6_4	141	142	A40c, caudal area 40(PFm)	-56, -49, 38	57, -44, 38
		IPL_L(R)_6_5	143	144	A39rv, rostroventral area 39(PGa)	-47, -65, 26	53, -54, 25
		IPL_L(R)_6_6	145	146	A40rv, rostroventral area 40(PFop)	-53, -31, 23	55, -26, 26
	Pcun, Precuneus	PCun_L(R)_4_1	147	148	A7m, medial area 7(PEp)	-5, -63, 51	6, -65, 51
		PCun_L(R)_4_2	149	150	A5m, medial area 5(PEm)	-8, -47, 57	7, -47, 58
		PCun_L(R)_4_3	151	152	dmPOS, dorsomedial parietooccipital sulcus(PEr)	-12, -67, 25	16, -64, 25
		PCun_L(R)_4_4	153	154	A31, area 31 (Lc1)	-6, -55, 34	6, -54, 35
	PoG, Postcentral Gyrus	PoG_L(R)_4_1	155	156	A1/2/3ulhf, area 1/2/3(upper limb, head and face region)	-50, -16, 43	50, -14, 44
		PoG_L(R)_4_2	157	158	A1/2/3tonIa, area 1/2/3(tongue and larynx region)	-56, -14, 16	56, -10, 15
		PoG_L(R)_4_3	159	160	A2, area 2	-46, -30, 50	48, -24, 48
		PoG_L(R)_4_4	161	162	A1/2/3tru, area1/2/3(trunk region)	-21, -35, 68	20, -33, 69
Insular Lobe	INS, Insular Gyrus	INS_L(R)_6_1	163	164	G, hypergranular insula	-36, -20, 10	37, -18, 8
		INS_L(R)_6_2	165	166	vIa, ventral agranular insula	-32, 14, -13	33, 14, -13
		INS_L(R)_6_3	167	168	dIa, dorsal agranular insula	-34, 18, 1	36, 18, 1
		INS_L(R)_6_4	169	170	vId/vIg, ventral dysgranular and granular insula	-38, -4, -9	39, -2, -9
		INS_L(R)_6_5	171	172	dIg, dorsal granular insula	-38, -8, 8	39, -7, 8
		INS_L(R)_6_6	173	174	dId, dorsal dysgranular insula	-38, 5, 5	38, 5, 5

Limbic Lobe	CG, Cingulate Gyrus	CG_L(R)_7_1	175	176	A23d, dorsal area 23	-4, -39, 31	4, -37, 32
		CG_L(R)_7_2	177	178	A24rv, rostroventral area 24	-3, 8, 25	5, 22, 12
		CG_L(R)_7_3	179	180	A32p, pregenual area 32	-6, 34, 21	5, 28, 27
		CG_L(R)_7_4	181	182	A23v, ventral area 23	-8, -47, 10	9, -44, 11
		CG_L(R)_7_5	183	184	A24cd, caudodorsal area 24	-5, 7, 37	4, 6, 38
		CG_L(R)_7_6	185	186	A23c, caudal area 23	-7, -23, 41	6, -20, 40
		CG_L(R)_7_7	187	188	A32sg, subgenual area 32	-4, 39, -2	5, 41, 6
Occipital Lobe	MVOcC, MedioVentral Occipital Cortex	MVOcC _L(R)_5_1	189	190	cLinG, caudal lingual gyrus	-11, -82, -11	10, -85, -9
		MVOcC _L(R)_5_2	191	192	rCunG, rostral cuneus gyrus	-5, -81, 10	7, -76, 11
		MVOcC _L(R)_5_3	193	194	cCunG, caudal cuneus gyrus	-6, -94, 1	8, -90, 12
		MVOcC _L(R)_5_4	195	196	rLinG, rostral lingual gyrus	-17, -60, -6	18, -60, -7
		MVOcC _L(R)_5_5	197	198	vmPOS,ventromedial parietooccipital sulcus	-13, -68, 12	15, -63, 12
	LOcC, lateral Occipital Cortex	LOcC_L(R)_4_1	199	200	mOccG, middle occipital gyrus	-31, -89, 11	34, -86, 11
		LOcC _L(R)_4_2	201	202	V5/MT+, area V5/MT+	-46, -74, 3	48, -70, -1
		LOcC _L(R)_4_3	203	204	OPC, occipital polar cortex	-18, -99, 2	22, -97, 4
		LOcC_L(R)_4_4	205	206	iOccG, inferior occipital gyrus	-30, -88, -12	32, -85, -12
		LOcC _L(R)_2_1	207	208	msOccG, medial superior occipital gyrus	-11, -88, 31	16, -85, 34
		LOcC _L(R)_2_2	209	210	lsOccG, lateral superior occipital gyrus	-22, -77, 36	29, -75, 36
Subcortical Nuclei	Amyg, Amygdala	Amyg_L(R)_2_1	211	212	mAmyg, medial amygdala	-19, -2, -20	19, -2, -19
		Amyg_L(R)_2_2	213	214	lAmyg, lateral amygdala	-27, -4, -20	28, -3, -20
	Hipp, Hippocampus	Hipp_L(R)_2_1	215	216	rHipp, rostral hippocampus	-22, -14, -19	22, -12, -20
		Hipp_L(R)_2_2	217	218	cHipp, caudal hippocampus	-28, -30, -10	29, -27, -10
	BG, Basal Ganglia	BG_L(R)_6_1	219	220	vCa, ventral caudate	-12, 14, 0	15, 14, -2
		BG_L(R)_6_2	221	222	GP, globus pallidus	-22, -2, 4	22, -2, 3
		BG_L(R)_6_3	223	224	NAC, nucleus accumbens	-17, 3, -9	15, 8, -9
		BG_L(R)_6_4	225	226	vmPu, ventromedial putamen	-23, 7, -4	22, 8, -1
		BG_L(R)_6_5	227	228	dCa, dorsal caudate	-14, 2, 16	14, 5, 14
		BG_L(R)_6_6	229	230	dlPu, dorsolateral putamen	-28, -5, 2	29, -3, 1
	Tha, Thalamus	Tha_L(R)_8_1	231	232	mPFtha, medial pre-frontal thalamus	-7, -12, 5	7, -11, 6
		Tha_L(R)_8_2	233	234	mPMtha, pre-motor thalamus	-18, -13, 3	12, -14, 1
		Tha_L(R)_8_3	235	236	Stha, sensory thalamus	-18, -23, 4	18, -22, 3
		Tha_L(R)_8_4	237	238	rTtha, rostral temporal thalamus	-7, -14, 7	3, -13, 5
		Tha_L(R)_8_5	239	240	PPtha, posterior parietal thalamus	-16, -24, 6	15, -25, 6
		Tha_L(R)_8_6	241	242	Otha, occipital thalamus	-15, -28, 4	13, -27, 8
		Tha_L(R)_8_7	243	244	cTtha, caudal temporal thalamus	-12, -22, 13	10, -14, 14
		Tha_L(R)_8_8	245	246	lPFtha, lateral pre-frontal thalamus	-11, -14, 2	13, -16, 7